Selective ^{15}N-labeling of the side-chain amide groups of asparagine and glutamine for applications in paramagnetic NMR spectroscopy

Chan Cao[1], Jia-Liang Chen[1], Yin Yang[1], Feng Huang[1], Gottfried Otting[2], and Xun-Cheng Su[1]*

1. State Key Laboratory of Elemento-Organic Chemistry, College of Chemistry, Collaborative Innovation Center of Chemical Science and Engineering (Tianjin) Nankai University, Tianjin 300071, China

2. Research School of Chemistry, Australian National University, Canberra ACT 0200, Australia

* Corresponding author

phone: +86 22 23500623

e-mail: xunchengsu@nankai.edu.cn

Abstract

The side-chain amide groups of asparagine and glutamine play important roles in stabilizing the structural fold of proteins, participating in hydrogen-bonding networks and protein interactions. Selective ^{15}N-labeling of side-chain amides, however, can be a challenge due to enzyme-catalyzed exchange of amide groups during protein synthesis. In the present study, we developed an efficient way of selectively labeling the side chains of asparagine, or asparagine and glutamine residues with [15]NH$_2$. Using the biosynthesis pathway of tryptophan, a protocol was also established for simultaneous selective ^{15}N-labeling of the side-chain NH groups of asparagine, glutamine, and tryptophan. In combination with site-specific tagging of the target protein with a lanthanide ion, we show that selective detection of ^{15}N-labeled side-chains of asparagine and glutamine allows determination of magnetic susceptibility anisotropy tensors based exclusively on pseudocontact shifts (PCS) of amide side-chain protons.

Introduction

Asparagine and glutamine residues play important roles in stabilizing proteins and protein-ligand interactions (Creighton 1993; Lesk 2001). NMR studies have obtained valuable information on the structure, dynamics, and physiological functions of proteins from the side-chain amides of asparagine and glutamine (Buck et al. 1995; Pervushin et al. 1997; Bertini et al. 2000; Cai et al. 2001; Mulder et al. 2001; Higman et al. 2004; Liu et al. 2006, 2007, 2008ab). Strategies for resonance assignments of side-chain amide groups generally rely on triple-resonance NMR experiments using ^{13}C and ^{15}N-labeled protein samples (Grzesiek and Bax 1993; Farmer and Venters 1996; Löhr and Rüterjans 1997; McIntosh et al. 1997; Cai et al. 2001). Measurements and assignments of these NMR signals are generally time-consuming. Moreover, the sensitivity of the requisite NMR experiments decreases with increasing protein size and perdeuteration is generally required for big proteins. If the protein can be reversibly unfolded to allow back-exchange of deuterium, the perdeuteration approach allows the assignment of the side-chain amides of asparagine and glutamine in proteins of high molecular weight. Without perdeuteration, IS-TROSY (isotope-selective transverse-relaxation-optimized spectroscopy) has been shown to detect the side-chain amides for proteins of a molecular mass up to 80 kDa (Liu et al. 2006, 2007). However, the experiment cannot discriminate between the side-chain resonances of asparagine and glutamine.

Improving the spectral resolution by selective ^{15}N-labeling of the side-chain amide resonances is important for their unambiguous assignment. Glutamine and glutamate are key intermediates in the biosynthesis of amino acids, causing redistribution of ^{15}N nuclei between different amino acids in the process of *in vivo* protein synthesis. ^{15}N-scrambling can be suppressed by cell-free protein synthesis, following chemical inactivation of pyridoxal 5'-phosphate (PLP)-dependent enzymes (Su et al. 2011). Selective ^{15}N-labeling of side-chain amides *in vivo*, however, remains a challenge. Selective ^{15}N-labeling of the side-chains of glutamine and asparagine by ^{15}NH$_4$ assimilation *in vivo* was first reported by Tate et al. (1992). This method was unable to discriminate between the side-chain NH$_2$ groups of asparagine and glutamine because of the complex metabolism in *E. coli*. The problem was partially overcome by using an auxotrophic strain of *E. coli* (JK120, AsnA$^-$, and AsnB$^-$), allowing the selective ^{15}N-labeling of the NH$_2$ group of glutamine side-chains (Vance et al. 1997). Transaminase-deficient or auxotrophic mutant strains, however, usually produce the proteins of interest only in low yields (Vance et al. 1997; Tong et al. 2008; Whittaker 2007).

Proteins with selectively isotopic labeled amino acids have been used with great success in biomolecular NMR studies (McIntosh and Dahlquist 1990; Waugh 1996; Etezady-Esfarjani et al. 2007; Kigawa et al. 1995; Tugarinov et al. 1996; Kainosho and Güntert 2010; Ozawa et al. 2004, Shi et al. 2004; Staunton et al. 2006; Sobhanifar et al. 2010; Takeuchi et al. 2010; Loscha and Otting 2013), but there has been no report on methods for selective ^{15}N-labeling of asparagine side-chains only. In the present study, a systematic study was performed to produce proteins with selectively ^{15}N-labeled asparagine side-chains *in vivo*. The new labeling strategy relies on the biosynthesis pathways of asparagine and allows discrimination between the ^{15}NH$_2$ NMR signals of the side-chain amides of asparagine and glutamine. Inspired by the successful performance of the ^{15}N-labeling protocol of asparagine side-chains, an efficient protocol for ^{15}N-labeling of asparagine and glutamine side-chains was devised too. Both isotope-labeling strategies provide high-quality ^{15}N-HSQC spectra of the proteins of interest without substantial ^{15}N isotope scrambling. Based on the biosynthesis pathway of tryptophan that derives the indole amine from the side-chain amide of glutamine (Radwanski and Last 1995), we also established an efficient way for simultaneous selective ^{15}N-labeling of the side-chain NH groups of Asn, Gln, and Trp. Remarkably, labeling degrees of greater than 80% in the target proteins could be achieved.

Paramagnetic NMR spectroscopy has become a powerful tool in structural biology (Bertini and Luchinat 1999; Bertini et al. 2002; Pintacuda et al. 2007; Clore et al. 2007; Otting 2010; Clore 2011; Keizers and Ubbink 2011). The magnetic susceptibility anisotropy ($\Delta\chi$) tensors of paramagnetic lanthanide ions provide valuable structural restraints for the determination of protein-protein and protein-ligand complexes. In view of the ease with which proteins with selectively ^{15}N-labeled side-chains of asparagine and glutamine can be made, we assessed the possibility of determining the $\Delta\chi$ tensors by using the PCSs of side-chain amide protons only. The strategy was evaluated using *E. coli* prolyl-*cis-trans* isomerase B, PpiB (Edwards et al. 1997), a protein containing eleven asparagine and six glutamine residues, which was site-specifically labeled with a lanthanide binding tag.

Materials and methods

Protein expression and purification

Protein expression used the high-cell-density method described previously (Marley et al. 2001) with modifications. For uniform and selective ^{15}N-labeling, bacterial cells were grown at 37 °C in 1 L

Luria broth rich medium shaken at 220 rpm. Once the optical cell density at 600 nm (OD_{600}) reached about 0.6, the cell culture was gently spun down at 3000 rpm for 5 min, the cells were washed with MilliQ water and then resuspended in 250 mL of minimal M9 medium (see below). The cells were allowed to recover by incubation for 20 min at 37 °C. Protein expression was subsequently induced by addition of isopropyl β-D-1-thiogalactopyranoside (IPTG) to a concentration of 0.5 mM. After about 5 h incubation, the cells were harvested and stored at -20 °C. It is important to limit expression times to less then 8 h to minimize isotope scrambling.

The in-house optimized M9 medium in high-cell-density method was composed of 160 mM Na_2HPO_4, 40 mM KH_2PO_4, 2 mM $MgSO_4$, 0.1 mM $CaCl_2$, and a trace metal mixture (Studier 2005), 0.1% ^{12}C-glucose, $^{15}NH_4Cl$, and amino acids as specified in Tables 1 and 2. The high concentration of phosphate was necessary to stabilize the pH in the high-density cell culture. The concentrations of $^{15}NH_4Cl$ and the amino acids Asp, Asn, and Gln were varied for optimal isotopic labeling yield.

NMR experiments

All NMR spectra of protein samples were recorded at 298 K on a Bruker AV600 NMR spectrometer equipped with a QCI cryoprobe. The protein samples were in 20 mM MES buffer at pH 6.4 unless mentioned otherwise.

Analysis of isotope labeling yield

Uniformly ^{15}N-labeled protein samples were prepared and ^{15}N-HSQC spectra recorded for protein concentrations of 0.02, 0.04, 0.06, 0.08, 0.10, 0.20, 0.30, 0.40, and 0.50 mM. The cross-peak volumes of side-chain amides in ^{15}N-HSQC spectra were integrated using the program Sparky (Goddard and Kneller 2008). The cross-peak volumes measured by NMR were linearly dependent on the protein concentration measured by UV absorption at 280 nm (Fig. S1). The calibration data of Fig. S1 were used to determine the concentration of selectively ^{15}N-labeled protein and the isotope labeling yield.

NMR measurements of the $[^{14}NH_4^+]/[^{15}NH_4^+]$ ratio in cell lysate

The frozen cell pellet was thawed, resuspended in 20 mL buffer (20 mM Tris-HCl, pH 7.6, 2 mM EDTA, 2 mM $MgCl_2$, 1 mM DTT, 0.5 mM PMSF), and sonicated on ice until a very low viscosity of the suspension was achieved. The supernatant was recovered by centrifugation. An 0.6 mL aliquot of the supernatant was collected, the pH adjusted to 2.5 with 3 M HCl, the precipitate spun down, and the

resulting solution was used to record a 1D ^{1}H NMR spectrum. The relative abundance of [^{15}NH$_4^+$] and [^{14}NH$_4^+$] inside the cell was analyzed by comparing the respective integrated proton NMR signals.

Site-specific labeling of PpiB K25C with a lanthanide binding tag

The lanthanide binding tag 4'-((pyridin-2-yldisulfanyl)methyl)-[2,2':6',2"-terpyridine]-6,6"-dicarboxylic acid (4MMTDA-Spy; Fig. 1; Su et al. unpublished results) was site-specifically attached to the K25C mutant of PpiB. A 0.6 mM solution of PpiB K25C was mixed with three equivalents of 4MMTDA-SPy in 20 mM MES at pH 6.4 at room temperature and the pH was adjusted to 6.5. The resulting mixture was incubated at room temperature for about 2 h. The final 4MMTDA-tagged protein was purified by anion exchange chromatography. The ligation yield was about 70%.

Results and Discussion

Selective ^{15}N-labeling of the side-chains of asparagine residues

As amino groups are transferred between glutamate, aspartate, glutamine, and asparagine by complicated metabolic inter-conversions, the side-chain amides of glutamine and asparagine tend to be labeled simultaneously, if ^{15}NH$_4$Cl is the sole nitrogen source (Table 1, entry a). It should be pointed out that strong amino scrambling was observed in ^{15}N-HSQC spectrum under low concentrations of glutamate and hence 2.0 g/L glutamate was maintained in this study. For selective ^{15}N-labeling of the side-chain amide of asparagine, the main steps in the biosynthesis of asparagine have to be taken into account. Firstly, ^{15}NH$_4^+$ assimilation by glutamate to create glutamine should be inhibited (Woolfolk et al. 1966; Stadtman 2001). Secondly, the metabolic conversion of glutamine to asparagine catalyzed by *Escherichia coli* asparagine synthetase B (AS-B) (EC 6.3.5.4) needs to be suppressed (Boehlein et al. 1994). Thirdly, the transformation of aspartate to asparagine should be retained (Cedar and Schwartz 1969). We recorded ^{15}N-HSQC spectra to quantify the ^{15}N-incorporation yield of side-chain amides in protein synthesis, using the calibration curves established with uniformly ^{15}N-labeled protein samples (Fig. S1). The average isotope-labeling ratio of different side-chain amides, $\bar{R}$, was calculated by comparison with the total protein concentration measured by UV absorption (Table 1).

The influence of unlabeled glutamine on ^{15}N-glutamine biosynthesis by ^{15}NH$_4^+$ assimilation of glutamate was verified (Table 1, entries a-d). As expected, the signals of ^{15}N-glutamine side-chain amides decreased with increasing ^{14}N-glutamine concentrations (Fig. S2, A-D). However, higher

concentrations of glutamine also resulted in lower ^{15}N-labeling yields of asparagine, which is probably caused by the following metabolic pathways: (i) high concentrations of glutamine increase the concentration of ^{14}NH$_4^+$ inside the cell through glutaminase (EC 3.5.1.2); (ii) high concentrations of glutamine decrease the ^{15}N-labeling of asparagine via asparagine synthetase B (AS-B) (EC 6.3.5.4). To verify these effects, we analyzed the relative intracellular abundance of ^{15}NH$_4^+$ and ^{14}NH$_4^+$ as a function of added ^{14}N-glutamine. We achieved this by recording 1D ^{1}H NMR spectra of the cell lysate (Fig S3). Under acidic conditions, the proton signals of ^{14}NH$_4^+$ and ^{15}NH$_4^+$ can readily be resolved in 1D NMR spectra (Fig. 2 and Fig S3). Integration of the respective multiplet components allows calculation of the [^{14}NH$_4^+$]/[^{15}NH$_4^+$] ratio. This showed that the intracellular [^{14}NH$_4^+$]/[^{15}NH$_4^+$] ratio increases with increasing ^{14}N-glutamine concentration in the outside feeding buffer (Table 1). When [^{14}NH$_4^+$] is abundant, it can be incorporated into ^{14}N-asparagine via asparagine synthetase A (AS-A) (EC 6.3.1.1). The side-chain amide of glutamine can also be directly transferred to asparagine by asparagine synthetase B (AS-B) (Huang et al. 2001). As shown in Table 1, the isotopic ^{15}N/^{14}N-labeling ratio of asparagine side-chains decreased from 62% to 35% with increasing concentrations of unlabeled glutamine in the medium (see also Fig. S2 and S4).

To improve the intracellular [^{14}NH$_4^+$]/[^{15}NH$_4^+$] ratio and the ^{15}N-labeling yield of asparagine side-chains, we turned to optimizing the concentrations of aspartate and ^{15}NH$_4^+$ in the M9 medium (Table 1 entries e-f). Increasing concentrations of aspartate and ^{15}NH$_4$Cl both decreased the intracellular [^{14}NH$_4^+$]/[^{15}NH$_4^+$] ratio and the ^{15}N-labeling yield of the asparagine side-chain amides improved significantly (Fig. S4). In addition, the NMR signals of ^{15}N-glutamine side-chains were completely suppressed. Up to 98% ^{15}N-labeling of asparagine side chains was achieved without any significant isotope scrambling (Table 1 and Fig. 3), however, it is not understood the true mechanism permitting the high ^{15}N-labeling yield of asparagine under abundant intracellular [^{14}NH$_4^+$].

Simultaneous selective ^{15}N-labeling of the side-chains of Asn and Gln residues

The high yield and selectivity of ^{15}N-labeling that can be achieved for asparagine side-chains enables discrimination of the NMR resonances of Asn and Gln side-chains in the ^{15}N-HSQC spectrum. In a second step, we developed an effective approach for simultaneously labeling the side-chain amides of Asn and Gln residues with ^{15}N *in vivo*. Unexpectedly, the ^{15}N-labeling yield for the Asn and Gln side-chains was boosted simply by replacing aspartate with asparagine using the same concentration of

$^{15}NH_4Cl$ (Table 2 entries a and c; Fig. 4). Table 2 also shows the effect of doubling the concentration of $^{15}NH_4Cl$ (entries a and b). Clearly, replacing aspartate by asparagine is the more efficient strategy. Using even more unlabeled asparagine further improved the isotopic labeling ratio, resulting in over 80% ^{15}N-labeling of the side-chains of asparagine and glutamine in the target protein (Table 2, entry d). Replacing aspartate by asparagine improved the $^{15}N/^{14}N$-labeling ratio by about 8% also in the presence of glutamine (Table S1). This may be explained by the common transport system for glutamate and aspartate, leading to mutual inhibition of transport even at μM concentrations (Kay 1971). This competition is relieved by replacing aspartate with asparagine. Owing to the rapid metabolism of asparagine in *E. coli* (Willis and Woolfolk 1974; Willis and Woolfolk 1975), the intracellular concentration of aspartate is thus more easily increased by the addition of asparagine instead of aspartate. Efficient transport of asparagine and conversion to aspartate is supported by the increase in intracellular $^{14}NH_4^+$ as suggested by the $[^{14}NH_4^+]/[^{15}NH_4^+]$ ratio (Table S1). It is remarkable that the $^{15}N/^{14}N$-labeling ratio of asparagine side-chain amides did not at all suffer from the addition of unlabeled asparagine, indicating that the ^{15}N-labeling yield of side-chain amides depends at least as strongly on the intracellular concentration of aspartate as on $^{15}NH_4^+$ (Fig. 4).

To validate the above labeling strategies, we expressed the N-terminal DNA-binding domain of the *E. coli* arginine repressor, ArgN (Sunnerhagen et al. 1997). Using the experimental conditions of entry f of Table 1, the asparagine side-chain amides were selectively ^{15}N-labeled to 82%. Using the conditions of entry d of Table 2, the side-chain amides of Asn and Gln were simultaneously ^{15}N-labeled with a labeling degree of up to 70% (Fig. S5). Neither case showed any evidence for significant ^{15}N-scrambling in the ^{15}N-HSQC spectra.

Selective ^{15}N-labeling of the side-chain NH groups of Asn, Gln, and Trp

The biosynthesis pathway of tryptophan includes anthranilate as an intermediate, which is synthesized from chorismate and glutamine by anthranilate synthase (EC 4.1.3.27), using the side-chain amide of glutamine as the nitrogen donor. Subsequently, the amino group of anthranilate ends up in the indole ring of tryptophan (Radwanski and Last, 1995). This pathway opens the possibility to ^{15}N-label the side-chains of glutamine, asparagine, and tryptophan simultaneously. As an example, we tested this labeling scheme with PpiB, which contains one tryptophan residue (Edwards et al. 1997). The labeling scheme used the conditions specified in entry d of Table 2, except that

tryptophan was omitted from the other amino acids.

Indeed, the ^{15}N-HSQC spectrum displayed six peak pairs of glutamine, twelve peak pairs of asparagine and a single cross-peak of the tryptophan side-chain (Fig. 5A and S6C), indicating that the tryptophan indole is ^{15}N-labeled via the glutamine metabolism with ^{15}NH$_4$Cl as the sole isotope source. Comparing the integrated cross-peak volumes between the protein samples produced with side-chain selective and uniform ^{15}N-labeling, we found isotopic labeling yields of 63, 59, and 55% for the side-chains of glutamine, asparagine, and tryptophan, respectively (Fig. 5A and Fig. S6). Notably, however, a limited amount of ^{15}N scrambling was observed. Most of the additional peaks were small (< 10% of the peak intensities observed for fully ^{15}N-labeled amides) and could be assigned to the backbone amides of aspartate, asparagine, glutamate, and glutamine, suggesting that they originated in the biosynthesis pathway of tryptophan. In general, these weak cross-peaks would hardly compromise the cross-peak identification of side-chain amides.

It is intriguing to note that the ^{15}N-labeling yield of the amino acid side-chains was in all examples greater than the [^{15}NH$_4^+$]/[^{14}NH$_4^+$] ratio measured for the cell lysate, suggesting that extra-cellular ammonium is directly transferred into the amino acid metabolism without prior equilibration with the cytoplasmic pool of ammonium ions. Indeed, NH$_3$ rather than NH$_4^+$ is thought to be the species transported across the *E. coli* cell membrane (Zhang et al. 2004).

Combining selective ^{15}N-labeling of side-chain amides with paramagnetic NMR

Measurements of pseudocontact shifts are particularly easy, if the spectral resolution is sufficient to allow unambiguous association of the cross-peaks in the paramagnetic sample with their corresponding partner in the diamagnetic reference by virtue of their displacement along diagonal lines in 2D NMR spectra (Bertini and Luchinat 1999; John and Otting 2007; Otting 2010). Usually, the fitting of Δχ tensors to protein structures relies on PCSs of protein backbone amide protons, since the backbone is more rigid than amino acid side-chains and thus presents more reliable coordinates. In protein systems of high molecular weight, however, the greater flexibility of side-chains combined with a usually low proton density around side-chain amides (as evidenced by the scarcity of NOESY cross-peaks typically observed for side-chain amides) makes them much easier to observe in ^{15}N-HSQC spectra than backbone amides. Therefore, we explored the feasibility of determining Δχ tensors by using only PCSs of side-chain amides.

We reacted the mutant K25C of PpiB with 4MMTDA-SPy for site-specific attachment of a paramagnetic lanthanide ion. The 4MMTDA tag (Fig. 1) is similar to the previously reported 4MTDA tag (Huang et al. 2013), which generates very large paramagnetic effects in protein NMR spectra. The 4MMTDA-SPy reagent spontaneously reacts with cysteine with formation of a disulfide bond. The ligation yield with PpiB K25C was about 70%. The protein-4MMTDA adduct was purified by FPLC using an anion exchange column. The ^{15}N-HSQC spectrum of the PpiB K25C-4MMTDA construct showed that the native cysteine residues Cys31 and Cys121, which are partially buried in the structure of PpiB, were not affected by the ligation reaction, indicating selective ligation of the cysteine in position 25 only. Addition of a paramagnetic lanthanide into the solution of K25C-4MMTDA produced significant chemical shift changes in the ^{15}N-HSQC spectra. The new cross-peaks were assigned to the paramagnetic species (Fig. 5B-D). The exchange between protein with and without paramagnetic lanthanide was slow. The complex of PpiB K25C-4MMTDA with Y^{3+} was used as the diamagnetic reference. PCSs of side-chain and backbone amide protons were measured as the chemical shifts of the sample with paramagnetic lanthanide ion minus the chemical shifts measured with diamagnetic Y^{3+}. For many asparagines and glutamines, the PCSs of their side-chain amide protons differed significantly between the c*is* and *trans* protons (Table S2). For example, the PCSs for the $H^{\varepsilon21}$ and $H^{\varepsilon22}$ protons of Gln97 in the complex of K25C-4MMTDA with Tm^{3+} were -0.49 and -0.38 ppm, respectively, showing that the side-chain is not sufficiently mobile to average the positions of the amide protons. For side-chain amide protons, seventeen PCSs were measured with Yb^{3+}, eighteen with Tm^{3+}, and fifteen with Tb^{3+}. These were used simultaneously with a common metal position to fit $\Delta\chi$ tensors to the crystal structure of PpiB (PDB ID: 2NUL; Edwards et al. 1997) using the program Numbat (Schmitz et al. 2008). Using the coordinates of the backbone amide protons, the solution structure of PpiB (PDB ID: 2RS4; Takeda et al. 2011) produced similar tensors as the crystal structure. As the conformations of the Asn and Gln side-chains are much less well defined in the NMR structure, we did not use it to fit $\Delta\chi$ tensors using only the PCSs of side-chain amide protons.

Fig. 6 shows the locations of the paramagnetic centers determined from the PCSs of the backbone and side-chain amide protons, respectively. Immobilization of the lanthanide ion may be aided by additional coordination to the side-chain carboxyl groups of Glu22 or Asp29, which reside in the same α-helix near the ligation site (residue 25). The paramagnetic center determined from the backbone amide PCSs (Table S3) was located 5.4 Å from the nearest carboxylate oxygen of Asp29. In view of

9

the discrepancies between the NMR and X-ray structures of PpiB in the loop regions, this $\Delta\chi$ tensor fit used only the PCSs of backbone amide protons in regions of regular secondary structure.

The asparagine and glutamine residues used to determine the $\Delta\chi$ tensors from side-chain amides are highlighted in Fig. 6. The metal position determined from the side-chain amides was 3.6 Å from the nearest carboxylate oxygen of Asp29. The correlations between back-calculated and experimental PCS data were good (Fig. S7 and S8). The tensor parameters are listed in Table 3.

Structure determinations of protein-protein and protein-ligand complexes by PCSs critically depend on the accuracy of the $\Delta\chi$ tensors. To compare the $\Delta\chi$ tensors derived from backbone and side-chain amides, we back-calculated the PCSs of the backbone amide protons using either the $\Delta\chi$ tensor derived from backbone amide protons, side-chain amide protons, or side-chain amide protons but using the metal position identified by the $\Delta\chi$ tensor derived from backbone amide protons. As expected, the correlation between the back-calculated and experimental PCSs was best, if the $\Delta\chi$ tensors derived from backbone amide protons were used (Fig. 7C). In contrast, the tensors derived from side-chain amide protons produced worse correlations (Fig. 7A), as expected if the conformations of the side-chains reported by the crystal structure are not perfectly conserved in solution. In addition, some of the PCSs of the side-chain amide protons included residues in less well-structured regions of the protein in order to maximize the number of PCSs. Improved correlations were obtained when $\Delta\chi$ tensors were determined from the PCSs of side-chain amide protons while the metal position was fixed to the site determined from the PCSs of the backbone amides (Fig. 7B). Notably, the axial components of the $\Delta\chi$ tensors determined in either fit were similar in magnitude.

Depending on the local structure environment, many amino acid side-chains are relatively rigid as determined by ^{15}N-{^{1}H} NOE and solvent accessibility measurements (Buck et al. 1995; Cai et al. 2001; Higman et al. 2004). Using the crystal structure of PpiB to calculate the solvent accessibility, the side-chains of N26, Q51, N70, N74, N78, Q97, N101, N105, and N109 are less than 20% solvent accessible in the crystal structure (Table S4). A large degree of immobilization is also supported by ^{15}N-{^{1}H} NOE measurements (Table S4) and by the different PCSs observed for the *cis* and *trans* protons of the side-chain amide protons mentioned above. Calculating $\Delta\chi$ tensors with only PCSs from side-chain amide protons by randomly sampling only 80% of the PCSs from all three sets of paramagnetic lanthanides in 100 fits indicated fairly good conservation of the principal axes of the $\Delta\chi$ tensors for each paramagnetic ion (Fig. S9).

Conclusions

Selective isotope labeling of proteins is a powerful technique for biomolecular NMR studies. Exploiting the biosynthetic pathways of asparagine and glutamine, the present work demonstrates that selective ^{15}N-labeling of the side-chains of asparagine, and of asparagine and glutamine residues, can be achieved in high yield with minimal ^{15}N-scrambling. This enables unambiguous identification of the cross-peaks of the side-chain amides of asparagine and glutamine in ^{15}N-HSQC spectra. In addition, selective ^{15}N-labeling of the NH groups of Asn, Gln, and Trp side-chains was also established.

The selective ^{15}N-labeling strategy for side-chain amides opens special opportunities for paramagnetic NMR spectroscopy. Detection of different PCSs for the *cis* and *trans* protons of a side-chain amide group immediately indicates that the side-chain experiences limited mobility. Those side-chains lend themselves particularly well to determinations of $\Delta\chi$ tensors, offering a promising approach to study protein-ligand complexes of high-molecular weight systems where the signals of side-chain amides are more easily detected than the resonances of backbone amides.

Acknowledgement

References

Bertini I, Luchinat C (1999) New applications of paramagnetic NMR in chemical biology. Curr Opin Chem Biol 3:145-151

Bertini I, Felli IC, Luchinat C (2000) Lanthanide induced residual dipolar couplings for the conformational investigation of peripheral ^{15}NH$_2$ moieties. J Biomol NMR 18:347-355

Bertini I, Luchinat C, Parigi G (2002) Paramagnetic constraints: an aid for quick solution structure determination of paramagnetic metalloproteins. Concepts Magn Reson 14:259–286

Boehlein SK, Richards NGJ, Schuster SM (1994) Glutamine-dependent nitrogen transfer in Escherichia coli asparagine synthetase B. J Biol Chem 269:7450-7457

Buck M, Schwalbe H, Dobson CM (1995) Structural determinants of protein dynamics: analysis of 15N NMR relaxation measurements for main-chain and side-chain nuclei of hen egg white lysozyme. Biochemistry 34:4041-4055

Cai M, Huang Y, Clore GM (2001) Accurate orientation of the functional groups of asparagine and glutamine side chains using one- and two-bond dipolar couplings. J Am Chem Soc 123:8642-8643

Cedar H, Schwartz JH (1969) The asparagine synthetase of *Escherichia coli* I. Biosynthetic role of the enzyme, purification, and characterization of the reaction products. J Biol Chem 244:4112-4121

Clore GM (2011) Exploring sparsely populated states of macromolecules by diamagnetic and paramagnetic NMR relaxation. Protein Sci 20:229-246

Clore GM, Tang C, Iwahara J (2007) Elucidating transient macromolecular interactions using paramagnetic relaxation enhancement. Curr Opin Struct Biol 17:603-616

Creighton, TE (1993) Proteins: structure and molecular properties, 2nd ed., Freeman, New York

Edwards KJ, Ollis DL, Dixon NE (1997) Crystal structure of cytoplasmic *Escherichia coli* peptidyl-prolyl isomerase: evidence for decreased mobility of loops upon Complexation. J Mol Biol 271:258-265

Etezady-Esfarjani T, Hiller S, Villalba C, Wüthrich K (2007) Cell-free synthesis of perdeuterated proteins for NMR studies. J Biomol NMR 39:229-238

Farmer BT, Venters RA (1996) Assignment of aliphatic side-chain ^{1}HN/^{15}N resonances in perdeuterated proteins. J Biomol NMR 7:59-71

Grzesiek S, Bax A (1993) Amino acid type determination in the sequential assignment procedure of uniformly ^{13}C/^{15}N-enriched proteins. J Biomol NMR 3:185-204

Goddard TD, Kneller DG (2008) Sparky 3, University of California, San Francisco

Higman VA, Boyd J, Smith LJ, Redfield C (2004) Asparagine and glutamine side chain conformation

in solution and crystal: a comparison for hen egg-white lysozyme using residual dipolar couplings. J Biomol NMR 30:327-346

Huang F, Pei YY, Zuo HH, Chen JL, Yang Y, Su XC (2013) Bioconjugation of proteins with a paramagnetic NMR and fluorescent tag. Chem Eur J 19:17141–17149

Huang XY, Holden HM, Raushel FM (2001) Channeling of substrates and intermediates in enzyme-catalyzed reactions. Annu Rev Biochem 70:149-180

Kay WW (1971) Two aspartate transport systems in *Escherichia coli*. J Biol Chem 246:7373-7382

John M, Otting G (2007) Strategies for measurements of pseudocontact shifts in protein NMR spectroscopy. ChemPhysChem 8: 2309-2313

Kainosho M, Güntert P (2010) SAIL – stereo-array isotope labeling. Q Rev Biophys 42:247-300

Keizers PH, Ubbink M (2011) Paramagnetic tagging for protein structure and dynamics analysis. Prog Nucl Magn Reson Spectrosc 58:88-96

Kigawa T, Muto Y, Yokoyama S (1995) Cell-free synthesis and amino acid-selective stable-isotope labelling of proteins for NMR analysis. J Biomol NMR 6:129-134

Lesk, AM (2001) Introduction to protein architecture: the structural biology of proteins. Oxford University Press, Oxford

Liu A, Li Y, Yao L, Yan H (2006) Simultaneous NMR assignment of backbone and side chain amides in large proteins with IS-TROSY. J Biomol NMR 36:205-214

Liu A, Yao L, Li Y, Yan H (2007) TROSY of side chain amides in large proteins. J Magn Reson 186:319-326

Liu A, Lu Z, Wang J, Yao L, Li Y, Yan H (2008a) NMR detection of bifurcated hydrogen bonds in large proteins. J Am Chem Soc 130:2428-2429

Liu A, Wang J, Lu Z, Yao L, Li Y, Yan H (2008b) Hydrogen-bond detection, configuration assignment

and rotamer correction of side chain amides in large proteins by NMR spectroscopy through protium/deuterium isotope effects. Chembiochem 9:2860-2871

Löhr F, Rüterjans H (1997) H$_2$NCO-E.COSY, a simple method for the sterospecific assignment of side-chain amide protons in proteins. J Magn Reson 124:255-258

Loscha KV, Otting G (2013) Biosynthetically directed ^{2}H labelling for stereospecific resonance assignments of glycine methylene groups. J Biomol NMR 55:97-104

Marley J, Lu M, Bracken C (2001) A method for efficient isotopic labeling of recombinant proteins. J Biomol NMR 20:71–75

McIntosh LP, Brun E, Kay LE (1997) Stereospecific assignment of the NH$_2$ resonances from the primary amides of asparagine and glutamine side chains in isotopically labeled proteins. J Biomol NMR 9:306-312

McIntosh LP, Dahlquist FW (1990) Biosynthetic incorporation of ^{15}N and ^{13}C for assignment and interpretation of nuclear-magnetic resonance spectra of proteins. Quart Rev Biophys 23:1-38

Mulder FA, Hon B, Mittermaier A, Dahlquist FW, Kay LE. (2002) Slow internal dynamics in proteins: application of NMR relaxation dispersion spectroscopy to methyl groups in a cavity mutant of T4 lysozyme. J Am Chem Soc 124:1443-1451

Ozawa K, Headlam MJ, Schaeffer PM, Henderson BR, Dixon NE, Otting G (2004) Optimization of an Escherichia coli system for cell-free synthesis of selectively ^{15}N-labelled proteins for rapid analysis by NMR spectroscopy. Eur J Biochem 271:4084-4093

Otting G (2010) Protein NMR using paramagnetic ions. Annu Rev Biophys 39:387-405

Pintacuda G, John M, Su XC, Otting G (2007) NMR structure determination of protein-ligand complexes by lanthanide labeling. Acc Chem Res 40:206-212

Pervushin K, Wider G, Wüthrich K (1997) Deuterium relaxation in a uniformly ^{15}N-labeled homeodomain and its DNA complex. J Am Chem Soc 119:3842-3843

Radwanski ER, Last RL (1995) Tryptophan biosynthesis and metabolism: biochemical and molecular genetics. The Plant Cell 7:921-934

Schmitz C, Stanton-Cook MJ, Su XC, Otting G, Huber T (2008) Numbat: an interactive software tool for fitting Δχ-tensors to molecular coordinates using pseudocontact shifts. J Biomol NMR 41:179-89

Shi J, Pelton JG, Cho HS, Wemmer DE (2004) Protein signal assignments using specific labeling and cell-free synthesis. J Biomol NMR 28:235−247

Sobhanifar S, Reckel S, Junge F, Schwarz D, Kai L, Karbyshev M, Löhr F, Bernhard F, Dötsch V (2010) Cell-free expression and stable isotope labelling strategies for membrane proteins. J Biomol NMR 46:33-43

Stadtman ER (2001) The story of glutamine synthetase regulation. J Biol Chem 276:44357-44364

Staunton D, Schlinker R, Zanetti G, Colebrook SA, Campbell ID (2006) Cell-free expression and selective isotope labelling in protein NMR. Magn Reson Chem 44:S2-S9

Studier FW (2005) Protein production by auto-induction in high-density shaking cultures. Protein Expr Purif 41:207-234.

Su XC, Loh CT, Qi R, Otting G (2011) Suppression of isotope scrambling in cell-free protein synthesis by broadband inhibition of PLP enymes for selective ^{15}N-labelling and production of perdeuterated proteins in H$_2$O. J Biomol NMR 50:35-42

Su XC, Otting G (2010) Paramagnetic labelling of proteins and oligonucleotides for NMR. J Biomol NMR 46:101-112

Sunnerhagen M, Nilges M, Otting G, Carey J (1997) Solution structure of the DNA-binding domain and model for the complex of multifunctional hexameric arginine repressor with DNA. Nat Struct Biol 4:819-826

Takeuchi K, Frueh DP, Sun ZY, Hiller S, Wagner G (2010) CACA-TOCSY with alternate ^{13}C-^{12}C labeling: a ^{13}C$^\alpha$ direct detection experiment for main chain resonance assignment, dihedral angle information, and amino acid type identification. J Biomol NMR 47:55-63

Takeda M, Jee J, Ono AM, Terauchi T, Kainosho M (2011) Hydrogen exchange study on the hydroxyl groups of serine and threonine residues in proteins and structure refinement using NOE restraints with polar side-chain groups. J Am Chem Soc 133:17420-17427

Tate S, Tate NU, Ravera MW, Jaye M, Inagaki F (1992) A novel ^{15}N-labeling method to selectively observe ^{15}NH$_2$ resonances of proteins in ^{1}H-detected heteronuclear correlation spectroscopy. FEBS Lett 297:39-342

Tugarinov V, Kanelis V, Kay LE (2006) Isotope labeling strategies for the study of high-molecular-weight proteins by solution NMR spectroscopy. Nat Protoc 1:749-754

Tong KI, Yamamoto M, Tanaka T (2008). A simple method for amino acid selective isotope labeling of recombinant proteins in E. coli. J Biomol NMR 42:59-67

Vance CK, Kang YM, Miller AF (1997). Selective ^{15}N labeling and direct observation by NMR of the active-site glutamine of Fe-containing superoxide dismutase. J Biomol NMR 9:201-206

Waugh DS (1996) Genetic tools for selective labeling of proteins with α-^{15}N-amino acids. J Biomol NMR 8:184-192

Whittaker JW (2007) Selective isotopic labeling of recombinant proteins using amino acid auxotroph strains. Methods Mol Biol 389:175-187

Willis RC, Woolfolk CA (1974) Asparagine utilization in *Escherichia coli.* J Bacteriol 118:231-241

Willis RC, Woolfolk CA (1975) L-asparagine uptake in *Escherichia coli.* J Bacteriol 123:937-945

Woolfolk CA, Shapiro B, Stadtman ER (1966) Regulation of glutamine synthetase: I. Purification and properties of glutamine synthetase from *Escherichia coli.* Arch Biochem Biophys 116:177-192

Zheng L, Kostrewa D, Bernèche S, Winkler FK, Li XD (2004) The mechanism of ammonia transport based on the crystal structure of AmtB of Escherichia coli. Proc Natl Acad Sci 49:17090-17095

Table 1. Experimental conditions used to produce ubiquitin with selectively ^{15}N-labeled side-chains of asparagine.

Entry	^{15}NH$_4$Cl (mM)	Glu (g/L)	Gln (g/L)	Asp (g/L)	Asn (g/L)	other aa[1] (g/L)	$[^{14}$NH$_4^+]/[^{15}$NH$_4^+]$ [2]	$\bar{R}_{Gln}$ [3] (%)	$\bar{R}_{Asn}$ [3] (%)
a	5	2	0	2	0	0.5	3.6	61	62
b	5	2	1	2	0	0.5	4.9	20	42
c	5	2	3	2	0	0.5	5.5	4	42
d	5	2	4	2	0	0.5	6.5	0	35
e	5	2	4	4	0	0.5	5.5	0	51
f	10	2	4	4	0	0.5	4.0	0	98

[1] All other amino acids except for glutamate, glutamine, aspartate, and asparagine.

[2] Intracellular relative abundance of $[^{14}$NH$_4^+]$ and $[^{15}$NH$_4^+]$ as determined by 1D ^{1}H NMR.

[3] Average percentage of ^{15}N-labeled side-chain amides as determined by the comparison of peak intensities in ^{15}N-HSQC and UV absorption spectra.

Table 2. Experimental conditions used to produce ubiquitin with selectively ^{15}N-labeled side-chains of glutamine and asparagine.[1]

Entry	[15]NH$_4$Cl (mM)	Glu (g/L)	Gln (g/L)	Asp (g/L)	Asn (g/L)	other aa (g/L)	$\bar{R}_{Gln}$ (%)	$\bar{R}_{Asn}$ (%)
a	5	2	0	2	0	0.5	61	62
b	10	2	0	2	0	0.5	75	82
c	5	2	0	0	2	0.5	76	77
d	5	2	0	0	4	0.5	84	85

[1] See footnotes of Table 1 for further details.

Table 3. $\Delta\chi$ tensor parameters of PpiB K25C-4MMTDA in complex with Yb^{3+}, Tm^{3+}, or Tb^{3+}.[1]

Ln^{3+}		$\Delta\chi_{ax}$ /10^{-32} m^3	$\Delta\chi_{rh}$ /10^{-32} m^3	α	β	γ
	a	7.9	4.9	153.2	99.2	103.6
Yb^{3+}	b	8.6	4.3	118.3	86.8	4.8
	c	7.2	0.7	121.9	97.2	30.9
	a	18.2	8.4	156.0	96.7	100.3
Tm^{3+}	b	19.9	0.7	132.5	87.9	103.1
	c	22.0	4.6	136.7	88.6	79.6
	a	-30.5	-17.2	156.9	97.3	100.9
Tb^{3+}	b	-31.5	-6.6	131.3	91.4	87.9
	c	-36.4	-13.7	137.3	89.9	83.1

[1] The tensor parameters were obtained by using the PCSs to fit $\Delta\chi$ tensors to the protein coordinates 2NUL (Edwards et al. 1997). The rows a to c refer to, respectively, using PCSs of only side-chain amide protons, using PCSs of backbone amide protons in regions with regular secondary structure, and using PCSs of only side-chain amide protons while keeping the metal fixed at the position determined in (b). Angles are in degrees.

Figure Legends

Fig. 1 Chemical structure of the lanthanide binding tag used in the present work, 4MMTDA-SPy.

Fig. 2 1D ^{1}H NMR spectra of ^{15}NH$_4$Cl and ^{14}NH$_4$Cl in cell lysate at pH 2.5. The ^{1}H NMR spectra A to F correspond to the cell lysates grown under the conditions a to f listed in Table 1, respectively. The spectra were recorded at 298 K at a ^{1}H NMR frequency of 600 MHz.

Fig. 3 Comparison of uniform ^{15}N-labeling and selective ^{15}N-labeling of asparagine side-chains. A) ^{15}N-HSQC spectra of uniformly ^{15}N-labeled ubiquitin (left) and ubiquitin with selectively ^{15}N-labeled asparagine side-chains (right). The spectra were recorded of 0.1 mM solutions of the double mutant A28C/K33N in 20 mM MES, pH 6.4, at a ^{1}H NMR frequency of 600 MHz. B) Cross-sections through the spectrum shown in A, highlighting the reduced signal overlap in the selectively labeled (solid lines) versus the uniformly labeled (dashed lines) sample.

Fig. 4 Comparison of uniform ^{15}N-labeling and selective ^{15}N-labeling of asparagine and glutamine side-chains. A) ^{15}N-HSQC spectra of uniformly ^{15}N-labeled ubiquitin (left) and ubiquitin with selectively ^{15}N-labeled asparagine and glutamine side-chains (right). The spectra were recorded of 0.1 mM solutions of ubiquitin A28C/K33N under the same conditions as in Fig. 3. B) Cross-sections through the spectra shown in A. Solid lines: uniform ^{15}N-labeling; dashed lines: selective ^{15}N-labeling of asparagine and glutamine side-chains.

Fig. 5 Pseudocontact shifts in a protein with selectively ^{15}N-labeled amino acid side-chains. A) Superimposition of ^{15}N-HSQC spectra of a 0.1 mM solution of uniformly ^{15}N-labeled PpiB (black) and PpiB with selectively ^{15}N-labeled side-chains of asparagine, glutamine, and tryptophan residues (red). B,C,D) Superimposition of ^{15}N-HSQC spectra of samples of PpiB-K25C-4MMTDA with selectively ^{15}N-labeled side-chains of glutamine, asparagine, and tryptophan, in complex with one equivalent of diamagnetic Y^{3+} (black) or the paramagnetic lanthanides Yb^{3+} (gold; B), Tm^{3+} (magenta; C), or Tb^{3+} (blue; D). The spectra were recorded at 298 K in 20 mM MES buffer, pH 6.4.

Fig. 6 Ribbon drawing of PpiB showing the metal positions determined by using the PCSs of backbone amide protons (black sphere) or of amide side-chain protons (blue sphere) to fit $\Delta\chi$ tensors to the

crystal structure of PpiB (PDB ID: 2NUL). Distances between the metal positions, and between the metal positions and the side-chain oxygen of Asp29 and the β-carbon of Lys25 are indicated. Side-chains with PCSs used for fitting Δχ tensors are labeled in red.

Fig. 7 Correlations between experimental PCSs (Exp_PCS) and back-calculated PCSs (Calc_PCS) for backbone amide protons in well-structured regions of PpiB. The Δχ tensors of Tb^{3+}, Tm^{3+}, and Yb^{3+} were fitted simultaneously using a common metal position. A) PCS back-calculation using the tensors obtained from the PCSs of side-chain amide protons only. B) PCS back-calculation using the tensors obtained from the PCSs of side-chain amide protons only, except that the metal center was fixed to the position of the Δχ tensor determined from PCSs of backbone amides. C) PCS back-calculation using the tensors obtained from the PCSs of backbone amide protons, using only residues in well-structured regions.
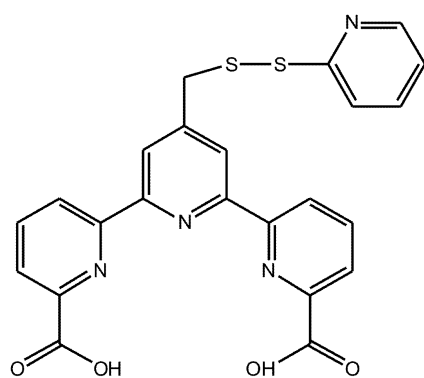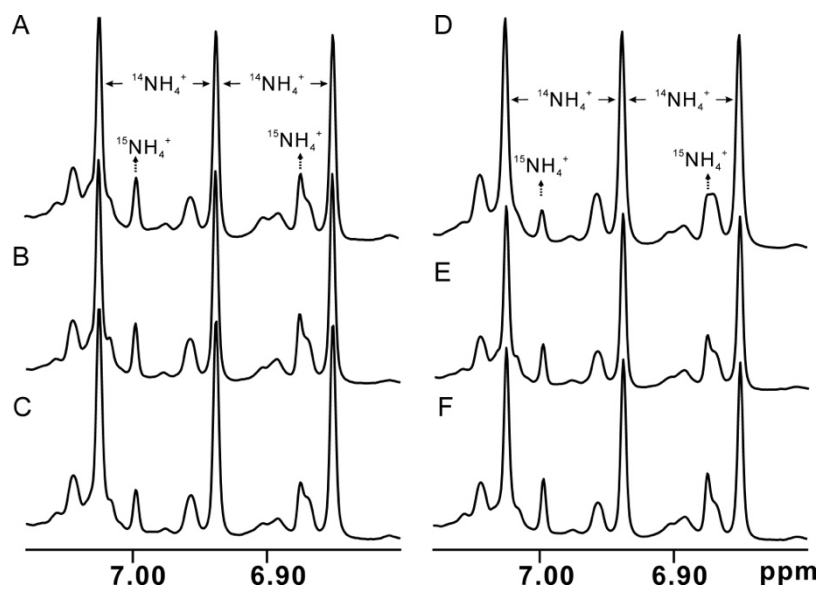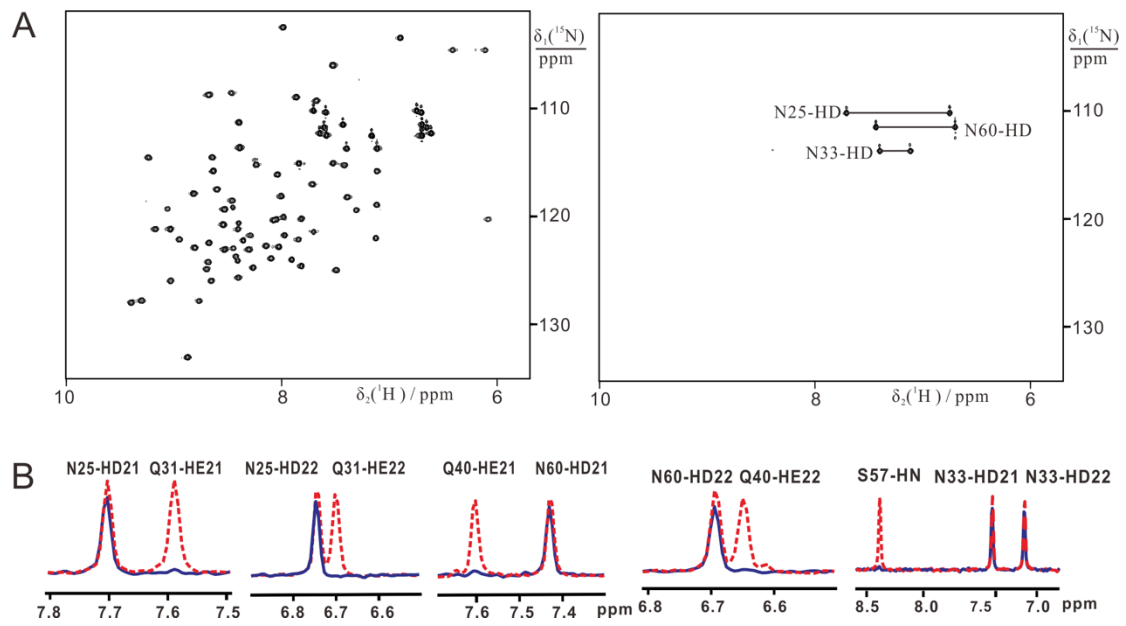
Fig. 1

Fig. 2
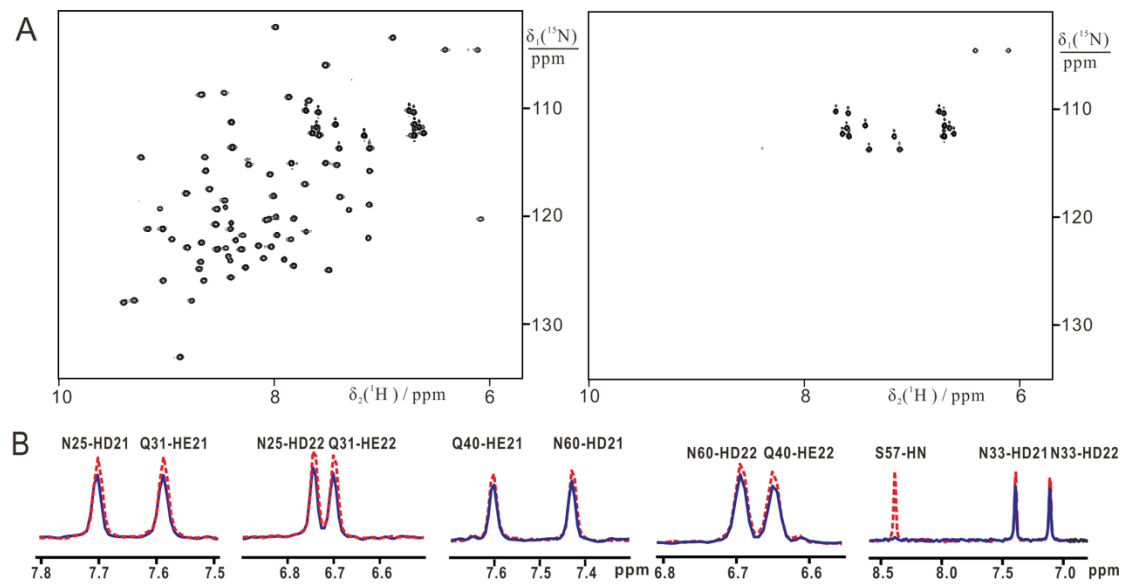
Fig. 3

Fig. 4

Fig. 5

Fig. 6

Fig. 7